Geotextiles and Geomembranes xxx (xxxx) xxx

Contents lists available at ScienceDirect

Geotextiles and Geomembranes

journal homepage: www.elsevier.com/locate/geotexmem

Performance of AC overlays using geogrids on PCC contraction joints

Muhammet Çelik [a], Mehmet Tevfik Seferoğlu [b,*], Muhammet Vefa Akpınar [c]

[a] Yalova University, Dept. of Civil Engineering, Turkey
[b] Gümüşhane University, Dept. of Civil Engineering, Turkey
[c] Karadeniz Technical University, Dept. of Civil Engineering, Turkey

ARTICLE INFO

Keywords:
Geogrid reinforcement
Accelerated pavement test
AC overlay
Contraction joints
Strain
Vertical displacement

ABSTRACT

It is widely known that vertical displacements and strains occur on the joints and these cause defects on the asphalt concrete (AC) overlays on existing Portland cement concrete (PCC) pavements. Various approaches were introduced to minimize these defects. In this study, the effect of joint support formed using the geogrid material with grout mortar on the vertical displacement of PCC and the strain at the bottom of the AC layer. Produced layers were exposed to 1,186,000 Equivalent Single Axle Load (ESAL) in an APT (Accelerated Pavement Test) facility and the results were monitored. According to the obtained results, the use of AC overlay reduces vertical displacement in the PCC by 75%. When geogrid reinforced AC overlay was used, an additional reduction in displacement by 41.2% was achieved. Geogrid reinforcement reduced strain values formed at the bottom of the AC layer from 29.5% to 92.5%. The use of geogrid at joints instead of increasing the thickness of the AC layer from 50 to 80 mm resulted a more significant reduction in both strain and displacement. Besides, the usage of a geogrid interlayer instead of increasing the thickness of the AC layer also provided a significant cost reduction of 57.9% in overall cost.

1. Introduction

Repeated traffic loads and climatic factors cause stress and strain on AC overlays. The microcracks, which are primarily responsible for the failure mechanism, usually start with tensile strain at the bottom of the asphalt layer. Various reinforcement materials such as chemical additives and geosynthetic products are used to increase the service life of the pavement (Seferoğlu et al., 2018; Sert and Akpinar, 2012). Geogrids, one of these geosynthetic products, are used in order to reduce the strains under the asphalt overlay and thus increase its life. There are some ongoing efforts to use geosynthetics as an interface before the application of AC overlays on existing concrete pavement that needs rehabilitation (Jordan et al., 2008; Khazanovich et al., 2009).

According to reports, strain formed at the bottom of the asphalt layer and resulting reflective cracks decrease the life span of the AC overlays (Beak et al., 2008). Vertical displacement which occurs on the joints or cracks in the concrete layer increases the strain rate causing reflective cracks (Hu et al., 2010). Strain values are observed at the bottom of the asphalt layer due to traffic loading and can cause both vertical displacement and cracking at the joint (Fig. 1).

Determining the strain values at the bottom of the asphalt layer is essential to predict the life span of the AC overlay. Generally, these predictions can be performed with two different methods. The first one is calculating the life span of the AC overlay by using strain values obtained in the theoretical model and formulas. However, each model or formula has its own assumptions regarding material properties, constitutive relationships, and load-bearing characteristics (Tabatabaee and Sebaaly, 1990). It is a widely known fact that the life span of the overlay calculated by these formulas cannot provide sufficient information for estimation of the actual life span of the overlay. (Beskou and Theodorakopoulos, 2011; Selvaraj, 2012). On the other hand, in the second method, the life span of the overlay is estimated by evaluating the changes in strain values developed by field conditions or repeated traffic loads at the facilities where the field conditions are demonstrated. Changes in strain values caused by the field conditions were monitored by the Long Term Pavement Performance (LTPP) Program. LTPP Program monitors the pavement performance data collected from gauges installed at various pavement test sections. Since obtaining data by LTPP Programs requires extensive timely testing, accelerated pavement testing (APT) facilities can be used in alternative. APT facilities provide

* Corresponding author.
E-mail addresses: m.celik53@gmail.com (M. Çelik), mtseferoglu@gmail.com, mtseferoglu@gumushane.edu.tr (M.T. Seferoğlu), mvakpinar70@yahoo.com (M.V. Akpınar).

https://doi.org/10.1016/j.geotexmem.2021.02.004
Received 13 February 2020; Received in revised form 9 January 2021; Accepted 19 February 2021

an economical and useful solution to evaluate the validity of mechanistic-empirical pavement design methods by demonstrating an environment similar to field conditions (White, 1989; Du Plessis et al., 2018). With these facilities, it is possible to collect data in a considerably short time period, in 3–5 months, which otherwise usually takes 8–10 years under field conditions (McNermey et al., 1994). The conditions created in the APT facilities can cause a change in the strain values. High temperature or heavy load in the APT facility increases the strain, additionally, asphalt type, thickness and aggregate properties change the strain characteristics of the pavements also (Xiaoming et al., 2012; Elseifi, 2009).

Geosynthetic reinforcements, primarily geogrid and others, have been widely used in pavement systems to prevent reflective crack in asphalt pavement layers. Several researchers in the past have been investigating the improvement in performance of pavement sections using geosynthetic materials (Sudarsanan et al., 2019; Kazimierowicz--Frankowska, 2020; Chen et al., 2018; Correia and Zornberg, 2018).

A number of studies have been reported on the use of geosynthetics and the intermediate layer in the application of the AC overlay for the rehabilitation of concrete. One of the first applications of geosynthetics was reported by Maurer and Malasheskie. They evaluated the effectiveness of geotextiles before the application of the AC overlay on the concrete roads build before 1940. However, in these earlier studies, two main difficulties were observed about the use of geotextile. The first one, the adhesive layer could not provide sufficient adhesion. The second is, geotextiles wrinkled and overlapped due to low adhesion and high friction (Maurer and Malasheskie, 1989).

Hu and Cao, carried out a study in the Xian province in China, attempting to prevent/delay fatigue crack by using different geosynthetics materials between concrete and asphalt overlay. The experiment results revealed that although the use of geosynthetics as an intermediate layer could reduce the shear resistance of asphalt, it could not prevent the formation of fatigue cracks sufficiently (Changshun and Dongwei, 1999). Another study was carried out by Button at Ozona, Texas, through an experimental setup using geosynthetics in a 400 m section of a continuously reinforced concrete pavement. Different types of geosynthetics were applied and any road deformations were monitored. Results obtained from this experiment suggested that the use of geosynthetics did not provide any additional prevention for fatigue crack growth on the AC overlays that will placed later. Therefore, it was concluded that thermal expansion and contraction in concrete pavements are responsible for the reflective cracks and geosynthetics cannot prevent these movements (Button, 1989). Shuler and Harmelink investigated the formation of reflective cracks by 8 different methods in the rehabilitation treatment for a road in Colorado. The results of this study pointed out that the use of geosynthetics can delay the formation of reflective cracks (Shuler and Harmelink, 2004). It has been concluded that the effect of different types of geosynthetic materials used in these studies varies depending on asphalt thickness, climate and reflection crack formation times. For this reason, it is necessary to continue studies to delay reflection cracking by using different types of geosynthetic materials.

In this paper, fiberglass geogrid and grout mortar layers applied to the half-joints in concrete pavements and covered by two types of AC overlay with different thickness in an APT facility. The load number and strain changes were monitored using strain gauges placed between the concrete and asphalt. The effectiveness of the geogrid reinforcement were examined by determining the relationships between vertical displacements, repeated load numbers and strain values. Another aim of this study was to estimate the economic effects of using geogrid materials and increasing the thickness of the asphalt layer. Therefore, a cost/benefit analysis is also presented in this paper for geogrid reinforcement and the thickness of the AC overlay.

2. Materials and method

The study was performed in an APT facility of Karadeniz Technical University (KTU). A moving wheel setup with 16 kN load capacity and capable of providing direct loads up to 15 km/h was used. The experiments were carried out with a 6.4 kN load up to 3 km/h. A half-axle and two-wheeled moving wheel setup were used (Fig. 2). The number of ESAL was used as the traffic volume unit. Applied loads were 30,000 ESAL per day and a total of 1,186,000 ESAL was completed in 3 months.

The experiments were carried out in a total of four different road sections, two sections per route (Table 1, Fig. 3) The dimensions of concrete layers were 4.00 × 2.00 m, separated by full joints and 60 mm

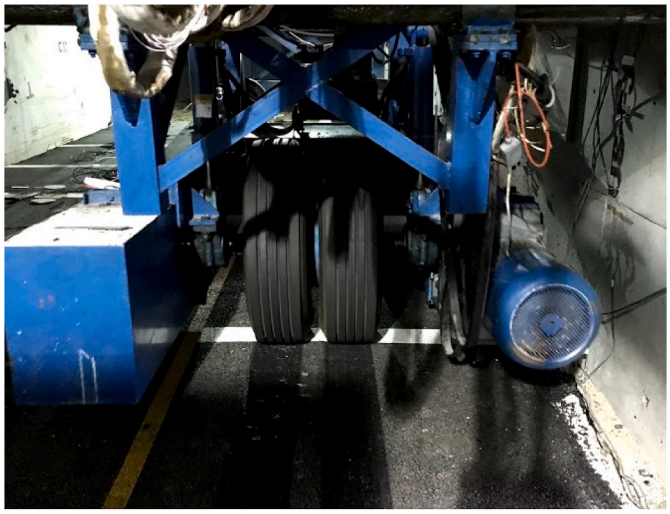

Fig. 2. Accelerated loading system.

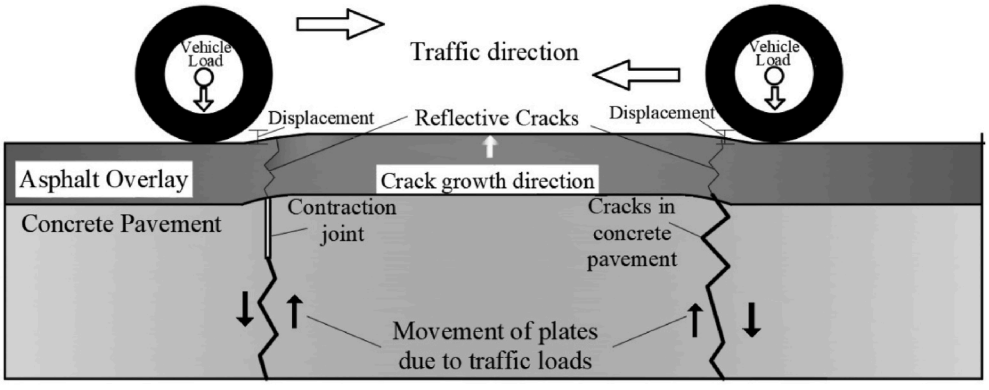

Fig. 1. Reflective cracks developed by the cracks in the joints or concrete pavement.

Table 1
Material characteristics of base, subbase and concrete pavement.

Layer	Thickness (mm)	Dry unit weight (kg/m^3)	Elastic Modulus (MPa)	CBR (%)	Moisture Content (%)	Relative Compaction (%)
Concrete	180	2.400	32.000	–	–	–
Base	300	2.100	300	80	5	98
Subbase	1000	1.900	100	60	6	95

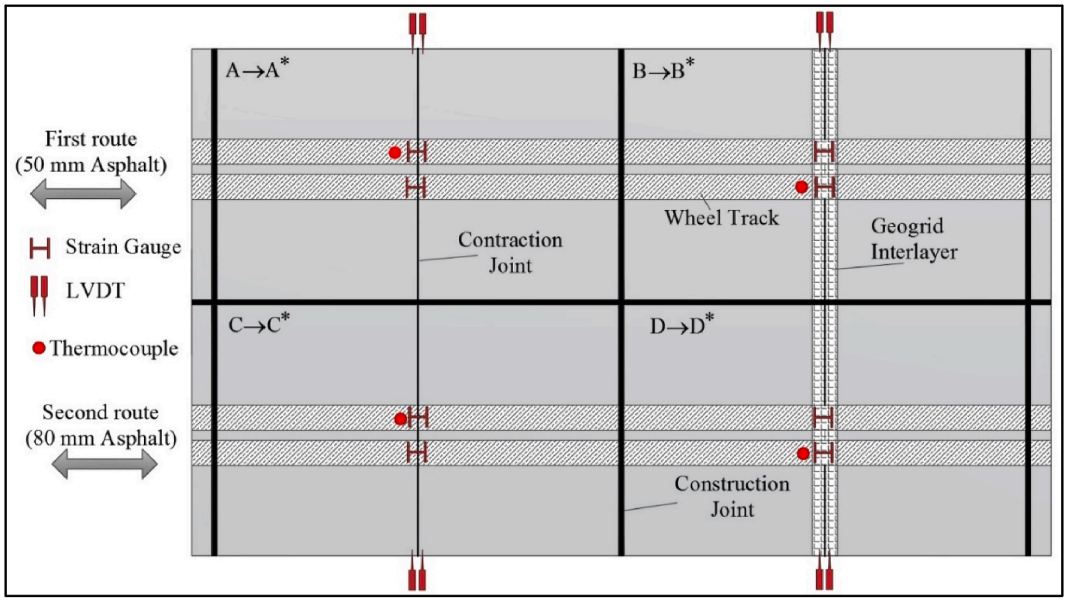

Fig. 3. Plan view of the experiment setup.

(1/3 of the layer thickness) half joint cut at the center of each layer. Each route was tested with 1,186,000 ESAL. The interior temperature of the facility and overlays were monitored by thermocouples during the experiments. The properties of the base, subbase and concrete pavement that the experiments carried out are given in Table 1. The types of layers used in the experiments are shown in Table 2.

Concrete layers were covered by two types of asphalt layers with different thicknesses; 1. Route: 50 mm and 2. Route: 80 mm. The asphalt layer was produced at a temperature of 163 °C and paved by Trabzon metropolitan municipality. The asphalt plant is located at a 3 km distance from the APT facility and transferred by municipality vehicles. The bitumen percentage in the asphalt mixture was 4.9% and the penetration value was varied between 50 and 70. The size distribution of the aggregates in the asphalt mixture was shown in Table 3. The cross-sections of the layer joints are given in Fig. 4.

The fiberglass geogrids reinforced with high-strength grout were used as an interlayer between concrete and asphalt (Fig. 5). The designed interlayer was chosen as a rigid structure with the property of high tensile stress. The interlayer was 8 mm thick, by 250 mm wide and the geogrid section consist of glass fiber. All geogrids had square apertures of 40 × 40 mm and 1.8 mm width and tensile strength of 90 kN/m. The mortar used was a high-strength self-consolidating mixture with 120 MPa compressive strength and 17 MPa bending strength.

The strain values were measured by H-type strain gauges and vertical displacements by the LVDT device. LVDT devices were placed on the left and right sides of the half-joints (Fig. 6a). A total of 8 LVDTs were used for four joints. The LVDTs provided vertical displacement measurements with a precision of 1/100 mm. Strain gauges were installed between concrete and asphalt layers, just below the wheels (Fig. 6b). Temperature and measurement ranges of the installed gauges were −34 °C to +175 °C, ±7500 μStrain, respectively.

The maximum and minimum values obtained by LVDTs during the loading tests were recorded and the difference value was calculated as the displacement movement. During the strain measurements, especially the tensile strain values, which have critical importance, were

Table 3
The size distribution of the aggregates in the asphalt mixture.

Sieve size	Retained (gr)	Retained, %	P%
1" (25.0 mm)	–	0.0	100.0
3/4" (19.0 mm)	0.0	0.0	100.0
1/2" (12.5 mm)	135.0	8.4	91.6
3/8" (9.5 mm)	330.0	20.5	79.5
No:4 (4.75 mm)	693.0	43.1	56.9
No:10 (2.00 mm)	1057.0	65.8	34.2
No:40 (0.425 mm)	1382.0	86.0	14.0
No:80 (0.180 mm)	1442.0	89.7	10.3
No:200 (0.075 mm)	1483.0	92.3	7.7

Table 2
Pavement types.

A	B	C	D	A*	B*	C*	D*
180 mm PCC	180 mm PCC	180 mm PCC	180 mm PCC	180 mm PCC+50 mm AC	180 mm PCC+50 mm AC + GR	180 mm PCC+80 mm AC	180 mm PCC+80 mm AC + GR

PCC: Portland cement concrete
AC: Asphalt concrete
GR: Geogrid reinforced

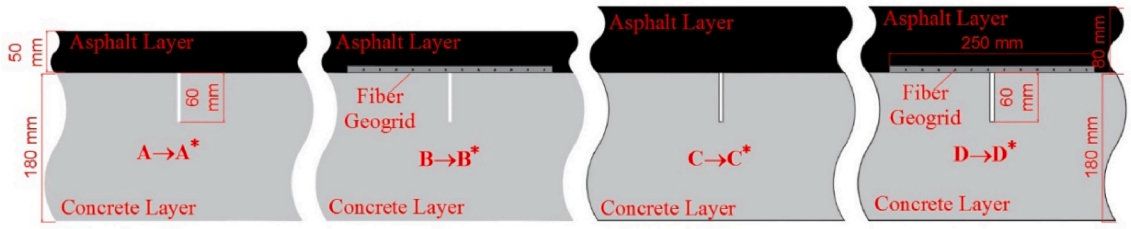

Fig. 4. The cross-sections of the four different joints loaded during experiments.

Fig. 5. Fiberglass geogrid and grout mortar application on contraction joint.

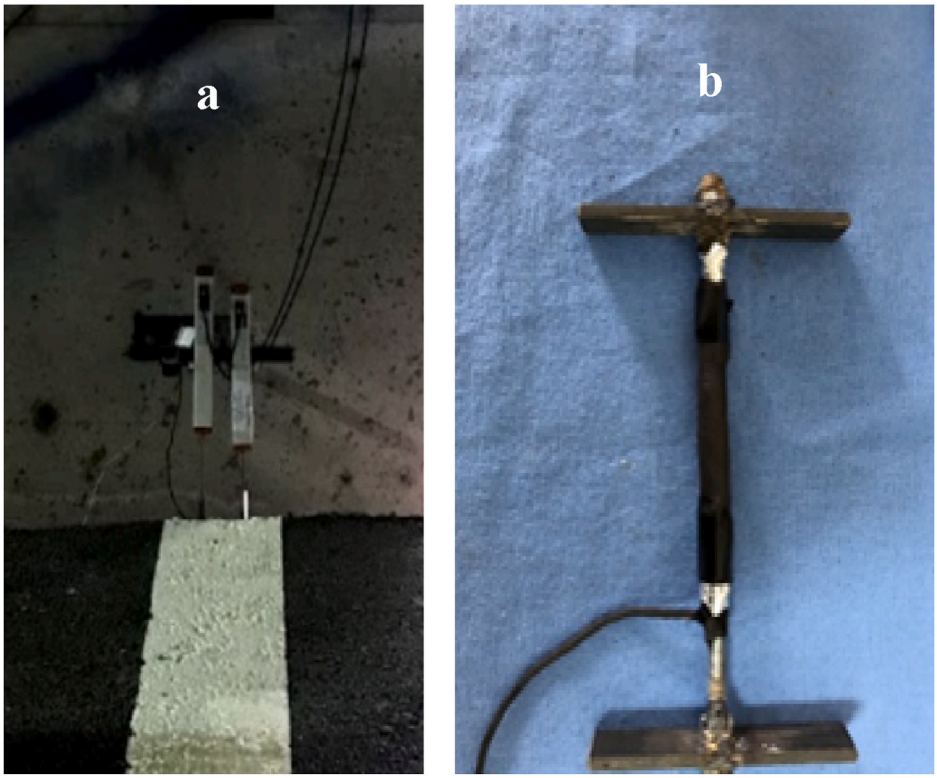

Fig. 6. The strain gauges and LVDT device used in the experiments.

monitored. The loading tests in the APT facility were completed in three months. The amount of the loads was maintained constant during the experiments.

In addition to the strain and vertical displacement values of the layers, a cost analysis was also performed on different types of cross-sections. During the cost analysis, item numbers (poses) used in Turkish institutions such as the General Directorate of Highways (KGM) and The Ministry of Environment and Urbanization (CSB) were used. Regarding the cost analysis of the geogrid interface that has no pose number, two different commercial poses and mould costs was formed by HPM 120 and TEX AR720. Commercial poses are determined according to the offer received from the manufacturer. The road platform width was accepted as 7 m and the length as 1 km for cost calculation. The distance of the asphalt plant to the aggregate crushing plant and the road

was determined as 15 km. The bitumen percentage was chosen as 5%, which is the prevalent ratio used in wearing and binder courses. The base, subbase and concrete pavement costs were accepted as the same in all comparisons. Finally, the AC overlay costs were calculated according to 50–80 mm thicknesses.

3. Results

3.1. Vertical displacements

The LVDT devices generated positive values when the wheels hit the edge of the layer and negative values at the center of the layer. The displacement value is equal to the absolute sum of positive and negative values. The vertical movement of the layers was estimated by total displacement values. The vertical displacement values of the concrete pavements (A, B, C and D) were measured before the application of the AC overlays in the APT facility. Then, the AC overlay with different thicknesses applied on these pavements and the vertical displacement values of new reinforced pavements (A*, B*, C* and D*) were measured (Fig. 7) The graph showing displacement changes as a result of the applied loads after the application of the AC overlay is shown in Fig. 8.

The vertical displacement values resulting from the applied loads are in the range of 0.31–0.34 mm. The fact that the displacement values of the concrete pavements are similar indicates the compaction degree of base layers are similar. Following the application of AC overlay and geogrid reinforcement, the displacement values in concrete joints decreased significantly by 75% compared to the displacement in concrete without AC overlay and geogrid. After the concrete pavement covered with only a 50 mm-thick asphalt layer, the displacement values decreased by 62.4%. When the thickness of the applied asphalt layer increased to 80 mm, a reduction of 70.24% in the displacement values was observed. While the geogrid reinforcement applied to a 50 mm-thick asphalt layer provided a reduction of 73.41% in the displacement values, this reduction improved to 90.8% when the thickness of the asphalt layer is increased to 80 mm.

It was observed that the vertical displacement values increased after the application of the AC overlay with the application of loads. When loading reached to 1,186,000 ESAL, the displacement value for the 50 mm thick asphalt layer decreased by 41.2%. This reduction is about 39.76% for the 80 mm thick asphalt layer. Overall, if the data presented in Figs. 7 and 8 are considered together, it is clear that the use of geogrid is more effective than increasing the thickness of the asphalt layer.

3.2. Strains

The strain observed at the bottom of the asphalt layer during the loading tests was monitored. The strain values were measured by strain gauges attached to concrete joints and routes of wheels. The tensile strain values, which are the critical strain values are presented in Table 5. Additionally, a graphical presentation of these results is given in Fig. 9. The highly sensitive strain gauges enabled monitoring even the

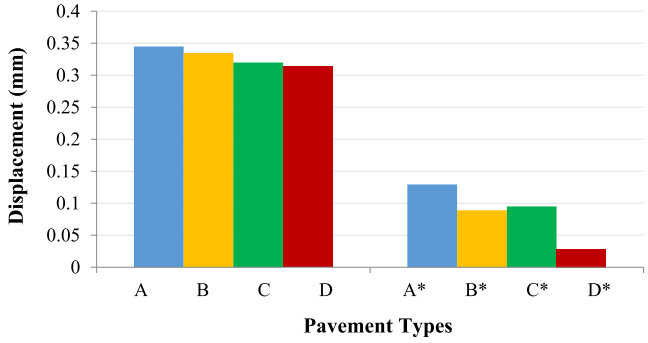

Fig. 7. Displacement value of different pavement types.

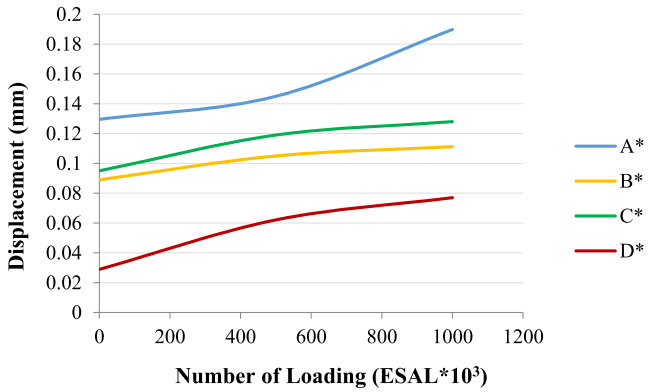

Fig. 8. The displacement trend after the application of AC overlays.

Table 5
Tensile strains in 50 mm and 80 mm-thick asphalt layers.

50 mm-thick asphalt layer			80 mm-thick asphalt layer		
Load	Unreinforced	Geogrid reinforced	*Load*	Unreinforced	Geogrid reinforced
ESAL × 10^3	ε × 10^{-6}	ε × 10^{-6}	*ESAL* × 10^3	ε × 10^{-6}	ε × 10^{-6}
0.475	150.893	164.04	0.475	92.5	16.71
71.16	197.145	172.52	71.16	65.02	16.25
83.02	164.63	145.42	83.02	61.36	27.47
100.81	189.58	130.98	100.81	50.83	12.36
136.39	200.35	145.73	136.39	53.41	22.43
177.9	171.61	133.17	177.9	110.52	20.83
237.2	142.87	108.17	237.2	108.47	21.98
355.8	145.85	109.25	296.5	105.95	5.95
593	156.61	111.73	355.8	112.1	10.53
830.2	163.94	113.16	474.4	115.26	20.15
1186	165.31	115.91	593	125.12	22.21
			830.2	127.73	9.61
			1186	125.49	13.28

lowest strain changes and remained functional during the experiments.

As shown in Fig. 9, one of the most attention-grabbing results is the unstable values observed at 200,000 ESAL; in other words, the observed strain values were spread out over a large range at this ESAL. This is because of the void ratio of the newly-paved asphalt. The asphalt layer, which was produced by Trabzon metropolitan municipality with a void ratio of 5%, continued to compact by the application of the first loads and the aggregate movements generated fluctuating (increasing and decreasing) strain values.

When the strain values were examined after the 1,186,000 ESAL were completed, the 80 mm-thick asphalt with geogrid displayed a 13.28 μStrain, this amount increased by 9.4 times to 125.49 μStrain if the geogrid interlayer not used. A similar behavior was observed for the 50 mm-thick asphalt, the use of the geogrid interlayer provided a significant reduction in strain values. Accordingly, while the measured strain value at the geogrid reinforced joint was 115.91 μ, this value increased by 42.6%–165.31 μStrain without geogrid.

As the effect of asphalt thickness on the strain values is examined at the sections without reinforcement, it was found that the 50 mm thick asphalt layer produced 31% more strain compared to the 80 mm thick asphalt. The strain values recorded for different layer types after 200,000 ESAL are plotted in Fig. 10.

The recorded strain values after 200,000 ESAL were varied between 25 and 165μStrain. These results are similar to the previous studies on AC overlays applied to half-joints. Özer et al. obtained strain values about 150–300 μStrain in a study on applying different adhesion materials for AC overlays on PCC (Özer et al., 2011). In another study carried out by Wolfe et al. strain values of the asphalt layer applied on different types of concrete were monitored and the obtained values were

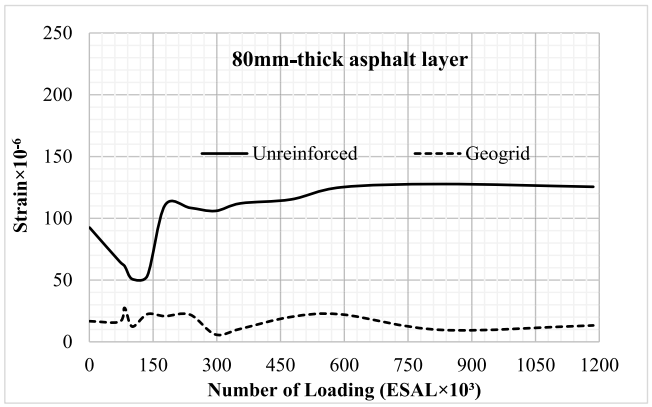

Fig. 9. Tensile strains formed at the bottom of the asphalt layer.

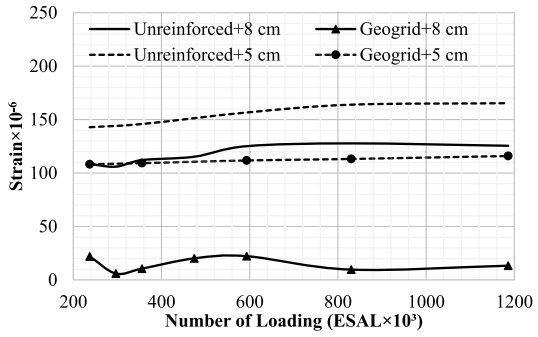

Fig. 10. Strain values recorded after 200,000 ESAL.

varied between 44–38 μStrain (Wolfe et al., 2009). Shippen broke an old concrete road, constricted it, and applied a 200 mm thick asphalt layer over the new structure. The obtained strain values at the bottom layer of the asphalt were varied between 20 and 120 μStrain (Shippen, 2005). Perez et al. placed metallic grids between asphalt and concrete and the obtained strain values at the bottom layer of the asphalt were varied between 10 and 80 μStrain level (Perez et al., 2007).

In the present study, it was demonstrated that increasing the thickness of AC overlays applied to PCC along with geogrid reinforcement had a significant effect on both reducing displacement and strain values. The best results recorded for the contraction joint were seen when using the 80 mm-thick asphalt layer with the geogrid interface. Moreover, it was found that the use of geogrid can provide some advantages even used in thin asphalt layers such as 50 mm. Further to that, it was suggested that the use of a geogrid interface under a 50 mm thick asphalt layer can exhibit better performance instead of using 80 mm thick asphalt without geogrid.

3.3. Cost comparison

Cost/benefit analysis is very important while designing pavement (Babashamsi et al., 2016). In this regard, different equations were developed for different types of pavement. A majority of formulas developed for asphalt pavement consider strain formation due to traffic loads. Since the fatigue cracks were examined in the current study, the critical strain values formed at the bottom of the asphalt layer were evaluated. The experimental strain values were used in the Asphalt Institute's equation (1982) and the allowable number of load repetitions, that is, the fatigue life was calculated (Asphalt Institute, 1982). The obtained results showed that the use of geogrid increased the lifespan of the road 3.43 times.

$$N_f = 0.0796\ (1/\varepsilon_t)^{3.291} * (1/E_1)^{0.854} \quad (1)$$

N_f: The allowable number of load repetitions to the failure by fatigue cracking
ε_t: Horizontal tensile strains at the bottom of the asphalt layer.
E_1: resilient modulus for a given temperature (calculated by a modification of resilient modulus with various equations and temperature).

Four different cross-sections were prepared for cost comparison and shown in Tables 6–8. The calculations were made according to the 50 mm and 80 mm thick asphalt layers and the cost of the geogrid interface was also taken into account separately. The width and thickness of the geogrid interfaces were accepted as 250 mm and 8 mm, respectively. It was considered that a 7 m-long geogrid interface is used every 5 m of the road. The calculations were made considering geogrid aperture size 40 × 40 mm, strength 90 kN/m and thickness 1.8 mm.

The cost of a geogrid interlayer for a 1 km road was calculated as approximately $3033. The cost of applying an 80 mm-thick asphalt layer instead of 50 mm is $7134.35 more expensive. Analysis conducted in this study showed that the use of a geogrid interlayer instead of

Table 6
Cost analysis of 50 mm-thick unreinforced binder layer (1 km road).

Ins.	Item Number	Item Description	Unit	Unit Price ($)	Amount	Cost ($)
KGM	GDH/ 4358	Heating of solid bitumen material in cisterns or tanks until absorption rate	ton	7.09	42	297.78
KGM	GDH/ 6305	Binder layer application for 50 mm thick 1 m^2 compacted asphalt concrete (Crash, eliminate, transfer, construct and compact)	m^2	1.39	7000	9730.00
ÇŞB	04.610/ 1B	Bitumen Price	kg	0.24	42,000	10,080.00
ÇŞB	NYF. Bitumen	Transfer from bitumen Kırıkkale refinery to the plant (660 km)	ton	17.11	42	718.62
ÇŞB	NYF.03	Transfer from HMA plant to the road (15 km)	ton	0.485	840	407.40
ÇŞB	NYF.03	Transfer from aggregate crushing plant to the plant (15 km)	ton	0.485	798	387.03
Cost of 5 cm *asphalt layer on ready-made base or concrete (VAT excluded)*			**TOTAL:**		**21,620.98 $**	

Table 7
Cost analysis of 80 mm-thick unreinforced binder layer (1 km road).

Ins.	Item Number	Item Description	Unit	Unit Price ($)	Amount	Cost ($)
GDH	GDH/ 4358	Heating of solid bitumen material in cisterns or tanks until absorption rate	ton	7.09	67.2	476.45
GDH	GDH/ 6305	Binder layer application for 80 mm thick 1m^2 compacted asphalt concrete (Crash, eliminate, transfer, construct and compact)	m^2	1.39	7000	9730.00
MEB	04.610/ 1B	Bitumen price	kg	0.24	67,200	16,128.00
MEB	NYF. Bitumen	Transfer from bitumen Kırıkkale Refinery to the plant (660 km)	ton	17.11	67.20	1149.79
MEB	NYF.03	Transfer from HMA plant to the road (15 km)	ton	0.485	1344	651.84
MEB	NYF.03	Transfer from aggregate crushing plant to the plant (15 km)	ton	0.485	1276.80	619.25
Cost of 8 cm *asphalt layer on ready-made base or concrete (VAT excluded)*			**TOTAL:**		**28,755.33 $**	

Table 8
Cost analysis of interface reinforcement (1 km road).

Ins.	Item Number	Item Description	Unit	Unit Price ($)	Amount	Cost ($)
Comm.	HPM 120	Cement-based, polymer-modified, single-component high-strength mortar containing silica fume	kg	0.33	6720	2217.6
Comm.	TEX AR720	Geogrid TEX ArR Glass Net 40 × 400 mm	m^2	1.64	350	574.00
ÇŞB	Y.21.001/ 02	Production of smooth concrete surface and concrete form from wood	m^2	7.58	28.00	212.24
Cost of 250 mm *width and* 8 mm *thick joints reinforcement (VAT excluded)*			**TOTAL:**		**3003.84 $**	

increasing the thickness of the asphalt layer reduced both strain and vertical displacement values. Moreover, the cost analysis calculations revealed that the use of geogrid interlayer instead of increasing the thickness of the asphalt layer 30 mm is 57.9% more economical. Consequently, it was suggested that applying geogrid interlayer under 50 mm thick asphalt layer with a 13.88% additional cost is preferable compared to using an 80 mm thick asphalt layer in terms of both strain and vertical displacement values.

During the service life of a road, the surface layer requires routine repair & maintenance. As a result of such repairs, the service life of the surface layer increases from 5 to 30 years (Jordan et al., 2008; Khazanovich et al., 2009) Moreover, previous studies indicated that the service life of road might decrease to 11 years if repair & maintenance works are not made (Shahin 2002). In the current study, the reflective cracks observed on the asphalt layer at joint locations were examined. In a study carried out at Wisconsin, it was stated that such cracks may occur in 1–2 years and the use of interlayers can delay the formation of such cracks by 42% (Makowski et al., 2005). Accordingly, we estimated the fatigue life using strain values and we found that the use of geogrid may increase the lifespan of the road by 3.43 times. The thin asphalt layers placed on the existing concrete pavement that examined in our study were used by Trabzon Metropolitan Municipality in the road network. The reflective cracks formed on the asphalt layer were fixed by filling with a special bituminous mortar to prevent leakage of water through cracks and crack propagation. The average road cost per kilometer was calculated in the present paper. It was estimated that the road without geogrid needs maintenance every two years. On the other hand, since the lifespan of the geogrid-reinforced roads are 3.43 times higher, it was considered that these roads require maintenance every 6.86 years. Accordingly, the cost of the crack filling repairs for a 1 km-road per two years was given in Table 9. The cost of the repair was based on the estimated cracks formed on 199 joints per 1 km road (one joint/5 m).

The cost of applying maintenances for 1 km road is $393.63. During its service life of 20 years, the road without geogrid needs 9 maintenances and its cost becomes $3544.74. However, geogrid-reinforced roads require only 3 maintenances. Therefore, it can be said that the use of geogrid is 3 times more economic.

4. Conclusions

When the AC overlay was constructed over the PCC pavement, the vertical displacement values in half-joint concrete layers decreased by 75%. Besides, increasing the thickness of the asphalt layer from 50 to 80 mm decreased the vertical displacement values by 33% and the use of a geogrid under the asphalt layer provided an additional reduction by 41.2%.

The tensile strain values at the bottom of the asphalt layer were monitored after placing the asphalt and the following results were obtained: The strain values of the asphalt layer were unstable in the first 200,000 ESAL. This unstable behavior indicates the compaction the newly-paved asphalt continues in the application of first loads. The results obtained after the 1,186,000 ESAL showed that increasing the thickness of the asphalt layer from 50 to 80 mm provided a reduction in strain values by 24%. Moreover, the use of geogrid provided an additional reduction ranging from up to 29.5–92.5%.

Table 9
Cost analysis of maintenance (1 km road (*200 joint*)).

Ins.	Item Number	Item Description	Unit	Unit Price ($)	Amount	Cost ($)
KGM	KGM/ 5020/K	Preparing the traffic signs and taking traffic safety measures	Day	93.08	1	93.08
KGM	KGM/ 4378	Cleaning concrete and all types of asphalt roads with sweeping machine	1000 m^2	3.323	0.2	0.6646
Comm.	Izofalt D	Filling bitumen including additive material and rubber (including labor and shipping costs)	25	1.66	200	332.00
The cost of repairing the reflective cracks 200 joint in 1 km *pavement (VAT not included)*			**TOTAL:**		**393.860 $**	

Evaluation of the strain and vertical displacement values suggested that the use of a geogrid interlayer instead of increasing the thickness of the asphalt layer is more favorable as it decreased both strain and vertical displacement values. Moreover, it was found that the use of a geogrid interlayer is a cost-beneficial approach, since increasing the thickness of the AC overlay by 30 mm (from 50 to 80 mm) increased the overall cost by 57.9%.

Acknowledgments

This research is part of a study being conducted at Karadeniz Technical University supported by the Scientific and Technological Research Council of Turkey (TÜBİTAK), Grant No: 217M481.

References

Asphalt Institute, 1982. 1982. Research and Development of the Asphalt Institute's Thickness Design Manual, Research Report, vols. 82-2. the Asphalt Institute.
Babashamsi, P., Yusoff, N., Ceylan, H., Nor, N., Jenatabadid, S.H., 2016. Evaluation of pavement life cycle cost analysis: review and analysis. Int. J. Pavement Res. Technol. 9.
Beak, J., Al-Qadi, I.L., Buttlar, W.G., 2008. In: Reflective Cracking Control, Illinois Bituminous Paving Conference, Illinois, USA.
Beskou, N.D., Theodorakopoulos, D.D., 2011. Dynamic effects of moving loads on road pavements: a review. Soil Dynam. Earthq. Eng. 31, 547–567.
Button, J., 1989. Overlay Construction and Performance Using Geotextiles, Transportation Research Record No. 1248. National Research Council, Washington D.C.
Changshun, H., Dongwei, C., 1999. Structural study of asphalt concrete overlays on the existing Portland cement concrete pavement. J. Eastern Asia Soc. Transport. Stud. 3.
Chen, Q., Hanandeh, S., Abu-Farsakh, M., Mohammad, L., 2018. Performance evaluation of full-scale geosynthetic reinforced flexible pavement. Geosynth. Int. 25 (1), 26–36.
Correia, N.S., Zornberg, J.G., 2018. Strain distribution along geogrid-reinforced asphalt overlays under traffic loading. Geotext. Geomembranes 46 (1), 111–120.
Du Plessis, L., Ulloa-Calderon, A., Harvey, J.T., Coetzee, N.F., 2018. Accelerated pavement testing efforts using the Heavy Vehicle Simulator. Int. J. Pavement Res. Technol. 11 (4), 327–338.
Elseifi, M., 2009. Analysis of Seasonal Strain Measurements in Asphalt Materials under Accelerated Pavement Testing and Comparing Field Performance and Laboratory Measured Binder Tension Properties. Report No. FHWA/LA. 09/444. Louisiana Transportation Research Center.
Hu, S., Zhou, F., Scullion, T., 2010. Reflection cracking-based asphalt overlay thickness design and analysis tool. J. Transport. Res. Board 1, 12–23.
Jordan, R.W., Coley, C., Harding, H.M., Carswell, I., Hassan, K.E., 2008. Best Practice Guide for Overlaying Concrete, Road Note RN41. Transport Research Laboratory, England.
Khazanovich, L., Rita, L., Tompkins, D., 2009. Guidelines for the Rehabilitation of Concrete Pavements Using Asphalt Overlays, Final Report. University of Minnesota.
Kazimierowicz-Frankowska, K., 2020. Influence of geosynthetic reinforcement on maximum settlements of semi-rigid pavements. Geosynth. Int. 27 (4), 348–363.
Makowski, L., Bischoff, D., Blankenship, P., Sobczak, D., Haulter, F., 2005. Wisconsin experiences with reflective crack relief projects. In: The 84th Annual Meeting of the Transportation Research Board. January.
Maurer, D., Malasheskie, G.J., 1989. Field performance of fabrics and fibers to retard reflective cracking. Geotext. Geomembranes 8 (3), 239–267.
McNermey, M.T., Hugo, F., McCullough, B.F., 1994. The Development of an Accelerated Pavement Test Facility for Florida Department of Transportation, CTR Research Report 997-3F. Center for Transportation Research, University of Texas.
Özer, H., Al-Qadi, L.I., Wang, H., Leng, Z., 2011. Characterization of interface bonding between hot-mix asphalt overlay and concrete pavements: modeling and in-situ response to accelerated loading. Int. J. Pavement Eng. 13 (2), 181–196.
Perez, S.A., Balay, J.M., Tamagny, P., Pelit, Ch, 2007. Accelerated pavement testing and modeling of reflective cracking in pavements. Eng. Fail. Anal. 14 (8), 1526–1537.
Seferoğlu, A.G., Seferoğlu, M.T., Akpinar, M.V., 2018. Experimental study on cement-treated and untreated RAP blended bases: cyclic plate loading test. Construct. Build. Mater. 182, 580–587.
Selvaraj, S.I., 2012. Review on the use of instrumented pavement test data in validating flexible pavement mechanistic load response models. Procedia Soc. Behav. Sci. 43, 819–831.
Sert, T., Akpinar, M.V., 2012. Investigation of geogrid aperture size effects on subbase-subgrade stabilization of asphalt pavements. Baltic J. Road Bridge Eng. 7 (2), 160–168.
Shahin, M.Y., 2002. Pavement Management for Airports, Roads and Parking Lots. Kluwer Academic Publishers, London.
Shippen, N., 2005. Measuring the Strain of the Road. Research Notes Oregon.
Shuler, S., Harmelink, D., 2004. Reducing Reflection cracking in asphalt pavements. In: 5th International RILEM Conference on Cracking in Pavements: Mitigation, Risk Assessment and Prevention, Colorado, pp. 451–458.
Sudarsanan, N., Karpurapu, R., Amirthalingam, V., 2019. Investigations on fracture characteristics of geosynthetic reinforced asphalt concrete beams using single edge notch beam tests. Geotext. Geomembranes 47 (5), 642–652.
Tabatabaee, N., Sebaaly, P., 1990. State-of-the-art Pavement Instrumentation. Transportation Research Record 1260. Transportation Research Board, Washington, D.C., pp. 246–255
White, T.D., 1989. Instrumentation and Pavement Design, Symposium on the State-Of-The-Art of Pavement Response Monitoring Systems for Roads and Airfields, Sponsored by U.S, vols. 89-23. Army Cold Regions Research and Engineering Laboratory, pp. 2–8. Report.
Wolfe, W., Butalia, S.T., Walker, H., 2009. Full-Dept Reclamation of Asphalt Pavements Using Lime-Activated Class F Fly Ash: Structural Monitoring Aspects. World of Coal Ash Conference, Lexington, USA.
Xiaoming, Y., Jie, H., Sanat, K.P., Chandra, M., Robert, L.P., Dov, L., Ha, Izhar, 2012. Accelerated pavement testing of unpaved roads with geocell-reinforced sand bases. Geotext. Geomembranes 32, 95–103.